Photochemistry and Photobiology, 2013, 89: 1127–1134

Stratification of the Radiation Field Inside a Photobioreactor During Microalgae Growth

Josue M. Heinrich[1,2], Ignacio Niizawa[1], Fausto A. Botta[1,2], Alejandro R. Trombert[2] and Horacio A. Irazoqui*[1,2]

[1]Institute for the Technological Development of the Chemical Industry (INTEC), Group of Innovation on Bio-processes Engineering, National Research Council (CONICET), University of Littoral (UNL), Santa Fe, Argentina
[2]Department of Biochemistry and Biological Sciences (FBCB), Group of Innovation on Bio-processes Engineering, University of Littoral (UNL), Santa Fe, Argentina

Received 12 April 2013, accepted 8 May 2013, DOI: 10.1111/php.12095

ABSTRACT

Light availability is a main issue in autotrophic growth of photosynthetic microorganisms. The change of the suspended cells concentration and that of their chlorophylls content during microalgal growth alters the optical properties of the aqueous suspension. This brings about changes in the properties of the radiation field inside the reactor. In this work, we have computed the evolution in time of the local volumetric rate of absorption of photons inside a photobioreactor by means of a Monte Carlo simulation algorithm previously developed. From this study, we have computed two operational variables that are useful tools for the analysis, performance comparison, optimization and scaling up of photobioreactors: the average rate of photon absorption and the volumetric distribution function of photons absorption rates. Based on these two variables, it is possible to systematically quantify the degree of stratification of the culture medium, which is a decisive aspect that hampers the reactor efficiency regarding the energy usage for biomass production.

INTRODUCTION

Microalgae are a large group of photosynthetic microorganisms capable of transforming inorganic compounds into organics, using energy from sunlight. They are used in such diverse areas as oil source for biofuels production (1–5), food manufacturing (6), in cosmetics and pharmaceutical industries (7), in CO_2 sequestration (8–10) and as a means for wastewater treatment in bioremediation (11).

Although some microalgae species can be grown as heterotrophs or as mixotrophs (12,13), autotrophic culturing techniques are mostly used. Light is the only source of energy for photoautotrophic growth, and it is well recognized that the algal growth kinetics and the biomass composition depend on the light availability as well as on its spectral composition (14–16). One of the difficulties hindering the expansion of the use of technologies based on microalgae culturing is the lack of reliable and validated methods for the design and scale up of suitable photobioreactors (PBRs), which should be able to bridge the distance from laboratory results to the required industrial scale. Because light availability has a critical effect on the biomass productivity of a microalgal culture, the efficient use of radiant energy is one of the main concerns when designing a PBR (17–19).

The simulation of the radiation field in microalgae cultures (20,21) requires knowing the absorption and scattering coefficients of the suspension, as well as the scattering phase function $B\left(\underline{\hat{\Omega}}' \cdot \underline{\hat{\Omega}}\right)$. These optical properties were determined in a previous work (22,23).

The optical properties change during microalgae culture. This is due to the increase in the suspension cell count or to changes in the size of the individuals, as well as to variations in the pigment composition of the medium. These modifications of the optical properties cause changes in the way the radiant energy is distributed inside the microalgae suspension. Thus, as the cultivation of microalgae progresses, cells face different lighting regimes that result from the change in optical properties, although the way in which the reactor is illuminated remains unchanged. The speed at which changes on the values of the optical parameters of the culture medium occur is an infinitesimal compared with the speed of light. Therefore, it is possible to assume that changes on the composition of the culture medium are followed by the radiation field properties without delay, evolving in time through a succession of steady states that follow the cell growth and related changes. The radiant energy field depends on time, not directly but through variations on the composition of the medium during the different phases of cellular growth.

The purpose of the present work was to present a particular procedure for the simulation of the radiation field in a PBR for microalgae culture, using Monte Carlo method, in view of optimization and scaling up of PBRs. The main objective consists in the application of the method to the analysis of the variation of the spatial distribution of the radiant energy density and to the spatial distribution of the local volumetric photon absorption rate inside PBRs during microalgae growth and metabolism. We describe how the cell growth changes the radiation field within the reactor by altering the availability of radiant energy and how these changes are related to the observed changes in microalgae growth rates.

MATERIALS AND METHODS

Strain and culture medium. A 500 mL volume of modified BBM (Bold's Basal Medium) medium containing an axenic inoculum of *Chlorella vul-*

*Corresponding author email: hirazo@santafe-conicet.gov.ar (Horacio A. Irazoqui)
© 2013 The American Society of Photobiology

garis (kindly provided by Dr. A.M. Gagneten, FHUC, UNL) with an $OD_{540} = 1$ (approximately) was used to inoculate 9.5 L of sterile BBM medium charged to the reactor. The culture was grown axenically at 25°C, illuminated with fluorescent light. Atmospheric air enriched with CO_2 (0.34%) and sterilized by filtration (0.45 μm pore size filter) was bubbled for the purpose of mixing; and to provide the medium with CO_2 as well as to avoid the accumulation of O_2 produced by photosynthesis. The original formulation of the BBM was modified so that the initial pH equals 7.

Biomass and chlorophyll concentration determinations. The algal mass concentration of the suspensions was determined by measuring the dry weight of the total suspended solids (TSS) (24). The algal mass contained in a 50 mL sample was retained by a 0.45 μm pore diameter filter, and then washed with 30 mL of distilled water and dried by heating at 100°C during 60 min. The dry weight of solids suspended in the suspension was calculated as the difference between the dry weight of the clean filter and that of the filter with the retained solids. The algal mass concentration was reported as the dry weight of suspended solids per unit volume of the sample. The total chlorophyll content of the suspensions was determined by the method reported by Ritchie (25). Aliquots of the samples were centrifuged to collect the suspended cells. Then, the cells were washed with distilled water and centrifuged once more. The harvested cells were suspended in methyl alcohol and the chlorophylls were extracted by heating the methyl suspension at 80°C during 5 min. The chlorophylls content was calculated from the values of light absorbance at 632, 652 and 665 nm wavelengths, using the absorbance coefficients reported in the study quoted above.

The reactor. An annular PBR was designed and built to perform experimental measurements and determine kinetic parameters that relate the light availability with the growth rate (Fig. 1). The reactor consists of two concentric glasses (both of 4 mm thickness and 310 mm height) with 50 and 250 mm of external diameter respectively. The useful volume of culture medium contained in the PBR was 10 L, which results in a liquid height of 220 mm, approximately. Due to its intrinsic symmetries, the annular geometry was chosen to facilitate the subsequent mathematical modeling. To supply the culture with CO_2; as well as to remove the O_2 produced by oxygenic photosynthesis and, at the same time, to promote mixing, the reactor was equipped with six air diffusers made of sintered glass. The reactor was connected to a culture platform Labfors3 (InforsHT, Switzerland) to control the air flow and the temperature of the suspension, and to register its pH and its pO_2. The air flow rate was kept at 0.3 vvm and the temperature at 25°C. The reactor was artificially illuminated all day long by means of a daylight fluorescent lamp (16W; Philips, Philips Argentina Sociedad Anónima, Buenos Aires, Argentina) of 26 mm external diameter, reaching a photon flux density over the internal glass tube of the reactor of 126 μmole photon s^{-1} m^{-2}. The transparent outer wall of the reactor was wrapped with a black blanket to isolate the microalgae suspension from the environmental light.

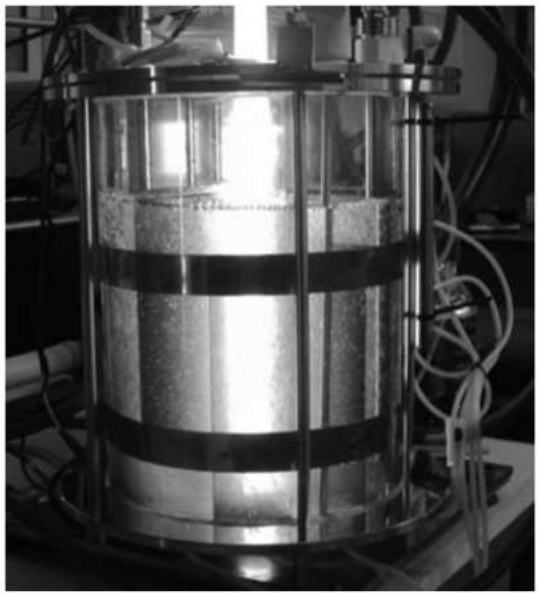

Figure 1. Photobioreactor designed and built for this application. It consists of a cylindrical annulus between two glass tubes, aligned coaxially to a daylight fluorescent lamp.

Simulation of the radiation field. The Monte Carlo method was employed to simulate the radiation field in the PBR. The procedure starts from the emission source. The emission of light by the lamp is superficial and isotropic (*i.e.* the intensity of the emitted light is independent of the direction of emission from any point on the lamp surface). Moreover, it is assumed that the lamp emits homogeneously throughout its entire surface. First, a position on the lamp surface is chosen randomly and both a direction and a wavelength are assigned to each emitted photon according to the emission characteristics of the radiation source. Successively, the trajectory of each photon among a sufficiently large number of them is simulated as it travels through each of the reactor sectors, until it reaches its eventual termination. Photons can be removed from the radiation field when they are absorbed by the microalgae suspension; when they impact on any opaque surface; or because they leave the reactor through the external glass wall. The reflection on the glass walls was modeled as that on an interface without thickness. The photon reflection on the reactor bottom and on its lid (both made on mirror-polished steel) was modeled as specular reflection. The effects of the probes and control devices (pH meter, O_2 sensor, cold finger, temperature sensor, sampling port, etc.) on the radiation field were neglected.

One by one, photons are emitted from the lamp in a succession, and in their way they undergo different events. Although the photons are emitted sequentially, it is important to keep in mind that all of them are simultaneous, and altogether simulate the radiation field distribution inside the reactor at every moment. This radiation field adjusts itself without delay to the evolution with time of the microalgae culture, following its changes in a permanent steady state. For the mathematical modeling, the simulation program was divided into 11 subroutines (shown in Fig. 2). Each subroutine is a mathematical model of the one of the events that photons can undergo on a border or within a particular sector of the reactor.

Symmetry condition. To simplify the program code and to reduce the simulation time, the reactor was divided into 12 symmetrical sectors, reducing the simulation to only one of these parts. Each sector comprises two contiguous regions of equal size: one of them with bubbles and the other bubble-free. The region above the diffuser is a homogeneous suspension of microalgae interrupted by air bubbles, homogeneously distributed within the volume of the section. Not all the bubbles have the same radius, but there is a radius distribution function instead, which depends on the air diffuser and on the liquid flow characteristics (26,27). The adjacent region consists in a homogenous microalgae suspension.

The probability of a collision between a photon and a bubble. The diffusers are trapezium-shaped porous slabs whose nonparallel edges coincide with the reactor radial direction, thus achieving an even distribution of bubbles in the volume of medium above them, irrespective of their diameter.

Above the air diffusers, the gas bubbles move upward through the homogenous algae suspension. Photons propagating in these sectors have chances of colliding against a bubble. When a photon originally moving through the homogeneous liquid suspension, encounters the liquid–air interface at a bubble surface, the photon can be reflected back to the liquid medium by changing its direction, or it can be refracted into the gas phase. Inside the bubble, the photon proceeds forward with its new direction until the air–liquid interface found ahead is reached. At this point, it can cross the interface and return to the culture medium after refraction, or reflected back to the inside of the bubble.

The probability that a photon encounters a bubble while traveling a distance s in the nonhomogeneous medium is computed as (see Supplementary Material: Eqs. S1–S6)

$$P(s) = \left|1 - \exp\left(-\frac{s}{\bar{s}_b}\right)\right| = \left\{1 - \exp\left|-\left(\frac{3}{4}\right)\theta_G \frac{s}{\bar{r}_b}\right|\right\} \qquad (1)$$

In Eq. (1), $\bar{s}_b$ is the average of the free flight distances of photons computed over the ensemble; $\bar{r}_b$ is the mean radius of the bubbles in the zone above each diffuser; $\theta_G = (2V_G/(V_L + V_G))$ is the gas volume fraction in the same zone; V_G is the total gas volume resident in the reactor and $(V_L + V_G)$ is the reactor total volume (28)

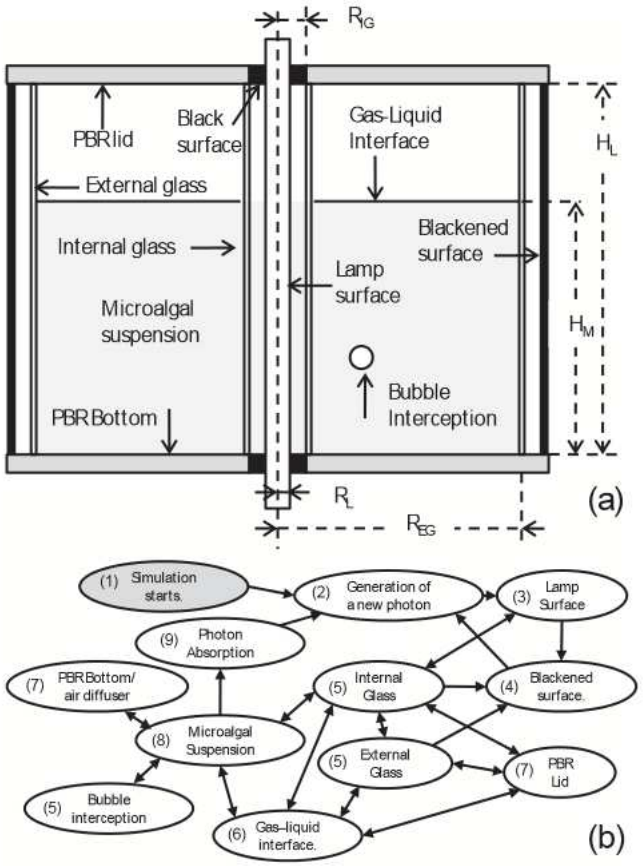

Figure 2. (a) Schematic of the photobioreactor. Photons are emitted from the fluorescent lamp surface. On their way, photons may undergo different events. When a photon is absorbed by microalgal cells in suspension or on the external black cover, a new photon is emitted. (b) Graph of the simulation algorithm. Every event that the photon may undergo is simulated by a different subroutine each one represented by a circle in the figure: (1) The time-changing absorption and scattering coefficient of the culture medium are set at every time. (2) A position on the lamp surface is randomly chosen for the emission of the photon; then a wavelength is assigned to the emitted photon according to the emission profile of the lamp. (3) A direction of motion is randomly assigned to the photon. (4) If the photon reaches a blackened surface, a new photon is generated. (5) Reflection or refraction on the glass surfaces is modeled according to Fresnel and Snell laws respectively. Each of the glass walls is modeled as two parallel interfaces separated from one another by the wall thickness (Heinrich et al. [22]). (6) Reflection or refraction on the gas–liquid interface is modeled according to Fresnel and Snell laws respectively. (7) The lid and the bottom of the reactor are modeled as mirror surfaces. The air diffusers were simulated as isotropic reflective surfaces. (8) The microalgal culture is modeled as a pseudo-continuum with centers of absorption or scattering randomly distributed throughout the suspension. (9) If photon absorption occurs, a unit is added to the corresponding counter. The local volumetric rate of photon absorption is computed for each wavelength at every position in the culture.

RESULTS AND DISCUSSION

Algal strain and culturing medium

The radiation field simulation in microalgae suspensions requires knowing the absorption and scattering coefficients and the phase function. These optical properties were determined in a previous work (22,23) and related to the biomass concentration and chlorophyll content. The evolution of biomass concentration with time is shown in Fig. 3a. The experimental results showed that the cellular chlorophylls concentration remained almost constant during the culture (15 days) at the average value of 2.4 mg Chl per 100 mg biomass.

The biomass concentration evolution with the time of culturing shows two different stages. In the first one (0–5 days), the cell concentration increases very slowly (Fig. 3a), due to the low concentration of biomass. In the second stage (starting on Day 5), the biomass concentration increases linearly and the growth rate remains almost constant.

Evolution of the optical parameters during microalgae culture

The bio-optical characteristics and biomass modify the optical properties of the microalgae suspension. Although the scattering phase function remains unchanged, the suspension absorption coefficient α_λ, as well as the scattering coefficient $\square_\lambda$, and consequently, the mean-free path of photons in the homogeneous suspension, $\bar{s}_{hs}$,

$$\bar{s}_{hs} = \frac{\int_0^\infty s e^{-(\alpha_\lambda+\xi_\lambda)\Delta s} ds}{\int_0^\infty e^{-(\alpha_\lambda+\xi_\lambda)\Delta s} ds} = \frac{1}{(\alpha_\lambda+\xi_\lambda)} \quad (2)$$

all these properties change with the biomass concentration, as it is shown in Fig. 4a and b, respectively, for wavelengths λ in the range from 400 to 700 nm, and for 1, 5 and 15 days of culturing.

With these parameters, and using the Monte Carlo simulation method, we can compute the local photon density function $n_\lambda\left(\underline{r}, \hat{\underline{\Omega}}, t\right)$. Due to the quantum nature of the radiant energy absorption, our analysis will be based on the local number density, $n_\lambda\left(\underline{r}, \hat{\underline{\Omega}}, t\right)$, of photons with energy (hc/λ), with trajectory through the position $\underline{r}$ in the direction $\hat{\underline{\Omega}}$. This is the suitable property of the radiant field on which to build a Monte Carlo algorithm. All other radiant field properties can be derived from this property (22,23). It is important remarking that the results obtained with this approach are equivalent to those obtained when the radiant energy field is modeled as an electromagnetic field. Moreover, the relationship between the basic field properties in these two approaches is as follows:

$$L_\lambda\left(\underline{r}, \hat{\underline{\Omega}}, t\right) = \frac{hc^2}{\lambda} n_\lambda\left(\underline{r}, \hat{\underline{\Omega}}, t\right) \quad (3)$$

In Eq. (3), $L_\lambda\left(\underline{r}, \hat{\underline{\Omega}}, t\right)$ is the intensity of the energy beam of wavelength λ, which is propagating in the direction $\hat{\underline{\Omega}}$ through the position $\underline{r}$.

The local volumetric rate of photon absorption

From $n_\lambda\left(\underline{r}, \hat{\underline{\Omega}}, t\right)$; the spectral density of photons which pass through each position $\underline{r}$, irrespective of the direction of their motion $\hat{\underline{\Omega}}$, is

$$n_\lambda(\underline{r}, t) = \int_{\hat{\underline{\Omega}}} d\hat{\underline{\Omega}} n_\lambda\left(\underline{r}, \hat{\underline{\Omega}}, t\right) = \int_0^{2\pi} d\phi \int_{-1}^{1} d\mu n_\lambda(\underline{r}, \mu, \phi, t) \quad (4)$$

If $n_\lambda(\underline{r}, t)$ is known, the local volumetric rate of photon absorption can be readily obtained:

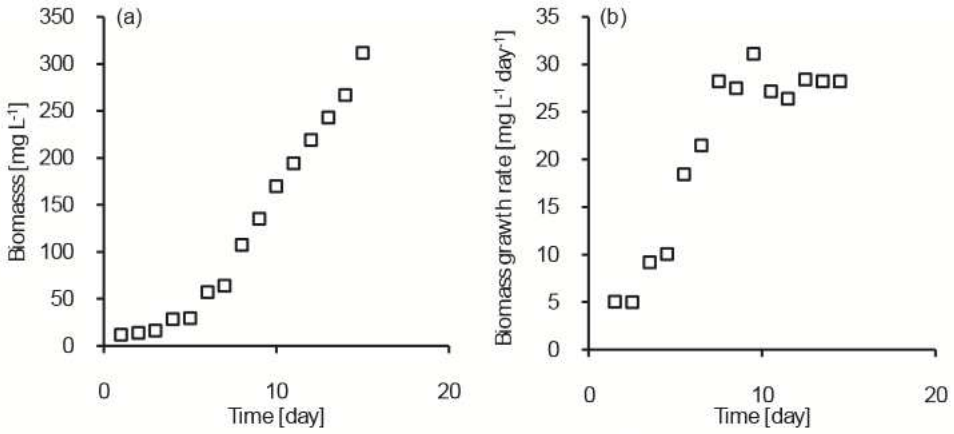

Figure 3. Results of the cultivation of microalgae. (a) Biomass concentration x [mg L^{-1}] as a function of time[*day*]. (b) Biomass growth rate, $r_x = \Delta x/\Delta t$ mg L^{-1} day^{-1} as a function of time [*day*].

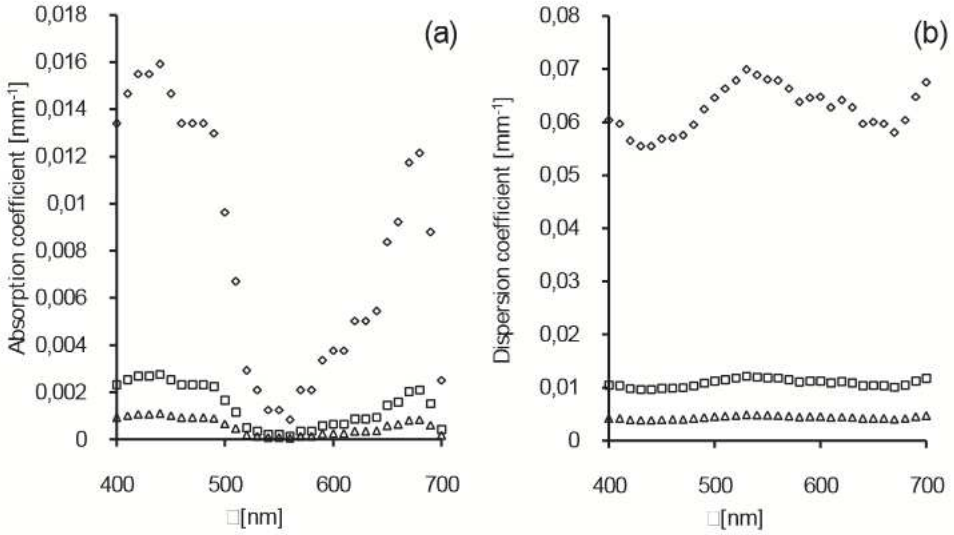

Figure 4. (a) absorption coefficient α_λ and (b) dispersion coefficient □$_\lambda$ *vs* wavelength λ in the range from 400 to 700 nm; for 1 (□), 5 (□) and 15 (□) days of culturing. The biomass concentrations measured in those days were 12, 30 and 312 mg L^{-1}, respectively.

$$r_\lambda^{abs}(\underline{r},t) = c\ \alpha_\lambda(t) n_\lambda(\underline{r}.t) \tag{5}$$

Knowing $r_\lambda^{abs}(\underline{r},t)$ at every location in the culturing medium is key to our understanding of the relative importance of different factors affecting light absorption by microalgae for a given reactor setup, and to compare the performance of different reactor configurations operating under different conditions, regarding this process. Not all the photons are equally absorbed in the suspension. Nor all reactor zones are equally productive regarding algae growth because their productivity depends on the local photon availability and on their wavelength. In Fig. 5, the rate of photon absorption is presented as a function of the radial distance, considering different wavelength intervals and different microalgae mass concentrations. Figure 5a–c illustrate $r_{VIS}^{abs}(\underline{r},t)$, $r_{540}^{abs}(\underline{r},t)$ and $r_{450}^{abs}(\underline{r}.t)$ corresponding to the intervals 400 □ λ □ 700 nm, 445 □ λ □ 455 nm and 445 □ λ □ 455 nm respectively. As can be seen, $r_{540}^{abs}(\underline{r},t)$is smaller than $r_{450}^{abs}(\underline{r},t)$ for all biomass concentrations.

Figure 5 shows that for 540 nm, the rate of absorption of photons is very low for all radial distances irrespective of the biomass concentration, whereas for 450 nm the absorption rate in the zones that are nearer to the irradiated boundary is higher than that in deeper zones of the suspension, and this difference increases with increasing biomass concentration. For high biomass concentrations, a large fraction of the photons that enter the suspension are absorbed in zones that are very close to the irradiated boundary and only a small fraction is left to be absorbed in more distant zones. In what to photon absorption rates is concerned, the biomass concentration is an important operating variable, which can be manipulated to balance the relative importance of deeper zones into the suspension, with the contribution of zones near the irradiated boundary, which will be reflected in that the profiles of rates of photon absorption will be less steep.

These differences in absorption rates of photons for different wavelengths could be an interesting parameter in PBRs operation conditions and design. In the case of concentrated suspensions, photons whose wavelength corresponds to the higher values of the absorption coefficient are absorbed in the zones closest to the irradiated boundary. As a consequence of this the deepest zones in a homogeneous suspension are relatively poorly illuminated by energy of high photosynthetic value. These regions, "darker" than the rest in what to energy useful for photosynthesis is

concerned, have a very low rate of photon absorption in the wavelength ranges of interest for photosynthesis, negatively affecting the performance of the equipment in terms of biomass productivity. The use of radiation sources of higher energy output is not an option without shortcomings because the increase of the availability of radiant energy in the zones of concentrated suspensions already exposed to high light intensity may cause the saturation of the photosynthetic systems, or even cause damage on them. In these situations, the selection of a radiation source emitting photons in wavelengths corresponding to a low or middle value of the absorption coefficient could overcome this problem.

The energy performance of PBRs: A methodology for its assessment, comparison and ranking based on the volume distribution according to the local rate of photon absorption

In the reactor, the local volumetric rate of photon absorption is not uniform. In a perfectly mixed reactor, the typical mixing time is much smaller than the typical time of growth. Under these conditions, the cells go from lighted zones to dark zones (and vice versa) many times before cellular replication occurs; thus, at a first glance, it could seem reasonable to assume that the kinetics of cell growth is driven by an average rate of photon absorption.

However, in a PBR with high cell density and illuminated with a high intensity of radiation, the cells could be subjected to oxidative stress conditions by being exposed to large photon densities in the zone adjacent to the irradiated boundary. On the other hand, in the barely lighted deeper zones of the suspension, the values of $r^{abs}_{VIS}(\underline{r}, t)$ may be smaller than the threshold value necessary for cell growth. In a situation like this, two reactors with the same average rate of photon absorption would have different observed yield of biomass produced per absorbed photon. Therefore, knowing $\bar{r}^{abs}_{VIS}(t)$ is not enough to fully characterize the reactor performance in what to energy usage is concerned.

To get round this problem, it is necessary knowing how the reactor volume is distributed among the $r^{abs}_{VIS}(\underline{r}, t)$ values in the range (0,□). That is why we introduce the notion of the volume distribution function $g(r^{abs}_{VIS}, t)$ among photon absorption rates $r^{abs}_{VIS}(\underline{r}, t)$.In terms of $g(r^{abs}_{VIS}, t)$ the average absorption rate, $\bar{r}^{abs}_{VIS}(t)$ μmol photons mm^{-3} s^{-1} is defined as follows:

$$\bar{r}^{abs}_{VIS}(t) = \frac{1}{V_L}\int_0^{\infty} r^{abs}_{VIS}(\underline{r}, t)\, g(r^{abs}_{VIS}, t)\, dr^{abs}_{VIS} \tag{6}$$

where $g(r^{abs}_{VIS}, t)$ is subjected to the normalization condition:

$$V_L = \int_0^{\infty} g(r^{abs}_{VIS}, t)\, dr^{abs}_{VIS} \tag{7}$$

In Eqs. (6) and (7), V_L is the liquid volume in the reactor and $g(r^{abs}_{VIS}, t) = dV_L/dr^{abs}_{VIS}$ is the volume distribution function in terms of photon absorption rates $r^{abs}_{VIS}(\underline{r}, t)$ in the reactor. With this tool at hand, we will propose a methodology to assess, compare and rank the energy performance of different reactors on a unique basis.

The cumulative probability $P(r^{abs}_{VIS}, t)$ of a cell reaching a position in a zone with its local volumetric rate of photon absorption included in the interval $(0, r^{abs}_{VIS})$ is equal to the ratio between the volume of that zone and the total volume of the PBR, and it can be computed in terms of $g(r^{abs}_{VIS}, t)$ as follows:

$$P(r^{abs}_{VIS}, t) = \frac{V(r^{abs}_{VIS})}{V_L} = \frac{1}{V_L}\int_0^{r^{abs}_{VIS}} g\left(r'^{abs}_{VIS}, t\right) dr'^{abs}_{VIS} \tag{8}$$

In Eq. (8), $V(r^{abs}_{VIS})$ is the reactor volume where $r^{abs}_{VIS}(\underline{r}, t)$ is in the range $(0, r^{abs}_{VIS})$. Among all possible values of r^{abs}_{VIS} in the range (0, □), we are interested in the values of r^{Q1}_{VIS}, r^{Q2}_{VIS} and r^{Q3}_{VIS}, corresponding to $V(r^{Q1}_{VIS}) = 0.25V_L$; $V(r^{Q2}_{VIS}) = 0.5V_L$; $V(r^{Q3}_{VIS}) = 0.75V_L$, respectively, where $V(r^{Q1}_{VIS})$, $V(r^{Q2}_{VIS})$ and $V(r^{Q3}_{VIS})$ represent the reactor volumes in which r^{abs}_{VIS} is in the range $(0, r^{Q1}_{VIS})$, $(0, r^{Q2}_{VIS})$ or $(0, r^{Q3}_{VIS})$. With these choices Eq. (8) turns into the following:

$$P(r^{Q1}_{VIS}, t) = \frac{V(r^{Q1}_{VIS})}{V_L} = \frac{1}{V_L}\int_0^{r^{Q1}_{VIS}} g(r^{abs}_{VIS}, t)\, dr^{abs}_{VIS} = 0.25 \tag{9a}$$

$$P(r^{Q2}_{VIS}, t) = \frac{V(r^{Q2}_{VIS})}{V_L} = \frac{1}{V_L}\int_0^{r^{Q2}_{VIS}} g(r^{abs}_{VIS}, t)\, dr^{abs}_{VIS} = 0.5 \tag{9b}$$

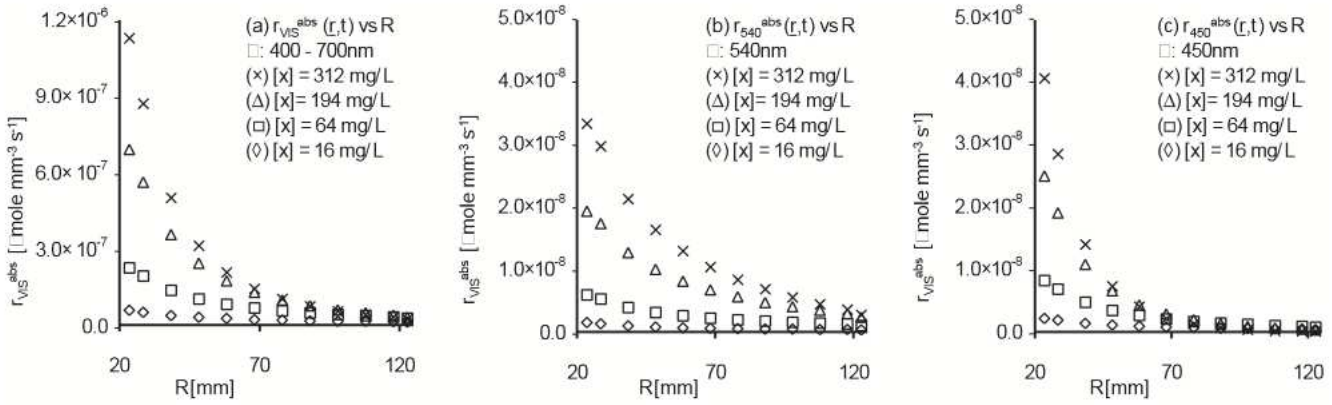

Figure 5. Local volumetric rate of absorption of photons [μmole photons s^{-1} mm^{-3}], *vs* the radial distance from the lamp axis, *R* (mm). For four different biomass concentrations: [*x*] = 16; 64; 194 and 312 mg L^{-1}. (a) r^{abs}_{VIS} for wavelengths λ in the range from 400 to 700 nm; (b) r^{abs}_{540} for 540 nm; and (c) r^{abs}_{450} for 450 nm. All the values correspond to H = 120 mm and $\phi_R = \pi/6$.

$$P(r_{VIS}^{Q3}, t) = \frac{V(r_{VIS}^{Q3})}{V_L} = \frac{1}{V_L}\int_0^{r_{VIS}^{Q3}} g(r_{VIS}^{abs}, t)\mathrm{d}r_{VIS}^{abs} = 0.75 \quad (9c)$$

In Fig. 6, $\bar{r}_{VIS}^{abs}(t)$ together with $r_{VIS}^{max}(t)$, $r_{VIS}^{min}(t)$, $r_{VIS}^{Q1}(t)$, $r_{VIS}^{Q2}(t)$ and $r_{VIS}^{Q3}(t)$ are plotted against the biomass concentration. In that figure, r_{VIS}^{max} and r_{VIS}^{min} represent the maximum and minimum values of $r_{VIS}^{abs}(\underline{r}, t)$, respectively, for each mass concentration.

In Fig. 6, it can be seen that initially the reactor operates with an almost evenly distributed rate of photon absorption, which is very low due to the low concentration of photosynthetic pigments. The low concentration of pigments which selectively absorb radiant energy according to its wavelength brings about that light reaches to every zone within the PBR. In this situation, the lowering of $r_{VIS}^{abs}(\underline{r}, t)$ with the radial distance is mainly due to the divergence of the energy beams. The concentration of pigments increases as the microalgae grow, and consequently also increases the rate of photon absorption. This leads to an ever growing stratification of the availability of light in the culture suspension. As microalgae concentration increases, the absorption of light in zones adjacent to the irradiated boundary also increases, while it decreases in deeper zones of the suspension. This phenomenon, widely known as *self-shading*, affects the performance of the equipment and becomes ever more abrupt with the increasing biomass concentration.

As it can be seen in Fig. 6, the average absorption rate of photons increases with the biomass concentration, reaching a value that remains almost constant. Also, the increment in the biomass concentration stratifies the reactor, as it can be concluded from the observed widening of the intervals defined by r_{VIS}^{min}, r_{VIS}^{max}, r_{VIS}^{Q1}, r_{VIS}^{Q2} and r_{VIS}^{Q3} for a given concentration. In other words, when the biomass concentration in the reactor exceeds the value of 100 mg L^{-1} a slight improvement in $\bar{r}_{VIS}^{abs}(t)$ is observed; however, this upturn is achieved at expense of a significant stratification of the reactor. From Fig. 6, it can also be seen that $\bar{r}_{VIS}^{abs}$ is almost equal to r_{VIS}^{Q3}. This indicates that almost the third part of the reactor is working with values of r_{VIS}^{abs} smaller than the value of $\bar{r}_{VIS}^{abs}(t)$.

This tool for the analysis of the energy performance of PBRs based on the simultaneous consideration of $\bar{r}_{VIS}^{abs}(t)$ and $g(r_{VIS}^{abs}, t)$ offers a common base to compare and to rank the efficiency of reactors of different configurations or of those working under different operating conditions. The kind of information derived from this method of analysis is of great help in the design and scaling up of PBRs.

To illustrate this, we have related the microalgae growth rate $r_x(t)$ [g L^{-1} d^{-1}] with the average absorption rate of photons $\bar{r}_{VIS}^{abs}(t)$ through a photon-to-biomass conversion yield $Y_{x/p}$ as in Eq. (10):

$$r_x(t) = Y_{x/p}\bar{r}_{VIS}^{abs}(t) \quad (10)$$

where $Y_{x/p}$ [mg μmole of Photons^{-1}] is the biomass generated per μmole of absorbed photons.

Figure 7 shows the evolution of $Y_{x/p}$ during the cultivation of microalgae. As we can see, the reactor performance varies according to a rather particular pattern: the value of $Y_{x/p}$ increases almost linearly during the early days of growing until the eighth day of culturing, when the biomass concentration reaches approximately 100 mg L^{-1}. From that day on, the value of $Y_{x/p}$ begins to decline in a linear fashion. Going back to Fig. 3b, we can see that at the same day, the biomass growth rate $r_x(t)$ ceases to increase linearly with time and becomes nearly a constant.

Because the dispersion of $r_{VIS}^{abs}(\underline{r}, t)$ around $\bar{r}_{VIS}^{abs}(t)$ increases with the biomass (Fig. 6), we can conclude that during the early days of cultivation, when biomass concentration is low and every zone in the suspension is well lit, the microalgae are able to use the captured light more efficiently. Later on, the average rate of absorption of photons increases during the early 8 days of culturing (See Fig. 3b), indicating that the number of total absorbed photons increases steadily resulting in greater efficiency in the total uptake of photons in the reactor. For greater concentrations of biomass, unequally illuminated zones appear and there is a correlative lowering of the efficiency of the usage of absorbed light. The biomass concentration continues growing but at a constant rate and therefore the reactor productivity does not change; more photons are absorbed without this leading to a greater rate of cell growth.

CONCLUSIONS

In this work, we have developed a simulator based on a Monte Carlo algorithm, which is able to predict the evolution of the local photon density function $n_\lambda(\underline{r}, \hat{\underline{\Omega}}, t)$. From $n_\lambda(\underline{r}, \hat{\underline{\Omega}}, t)$ is

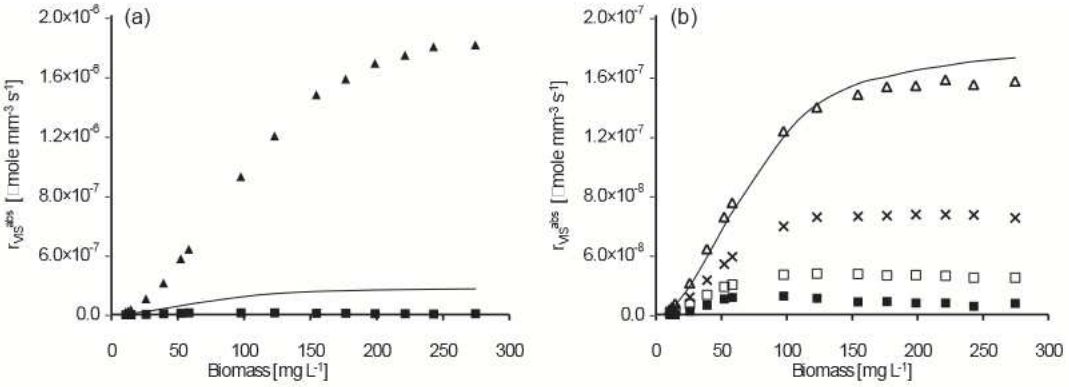

Figure 6. Average rate of photon absorption $\bar{r}_{VIS}^{abs}$ (including all photons with wavelength within the range of 400–500 nm and 600–690 nm) depending on the concentration of biomass attained during laboratory culturing [mg L^{-1}]. (a) (—): $\bar{r}_{VIS}^{abs}$; (□): r_{VIS}^{max}; (□): r_{VIS}^{min}. (b) (—): $\bar{r}_{VIS}^{abs}$; (□): r_{VIS}^{min}; (□): r_{VIS}^{Q1};(9): r_{VIS}^{Q2} and (□): r_{VIS}^{Q3}.

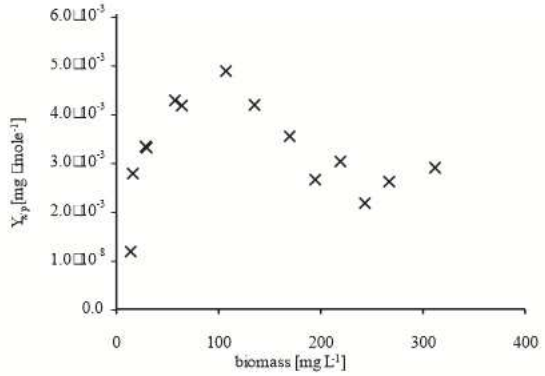

Figure 7. Yield $Y_{x/p}$ *vs* x. Calculated as $r_x(t)/\bar{r}_{PS}^{abs}(t)$, where $r_x(t)$ has units of mg L^{-1} dõa^{-1}, and $\bar{r}_{VIS}^{abs}(t)$ μmole photons L^{-1} dõa^{-1}.

possible to compute the local volumetric rate of photon absorption $r_{\lambda}^{abs}(\underline{r}, t)$. These properties depend on the position within the reactor, the wavelength and the biomass concentration. From $r_{\lambda}^{abs}(\underline{r}, t)$, we have calculated the average volumetric photon absorption rate $\bar{r}_{VIS}^{abs}(t)$ and the volume distribution function in terms of photon absorption rates, $g(r_{VIS}^{abs}, t)$, which are useful tools to estimate the light stratification inside the culture medium. The importance of the variables $\bar{r}_{VIS}^{abs}(t)$ and $g(r_{VIS}^{abs}, t)$ arises from the fact that they offer a simple procedure for the analysis, comparison and design of PBRs. By comparing the value of the variable $\bar{r}_{VIS}^{abs}(t)$ with the microalgae growth rate $r_x(t)$, we were able to compute the photon-to-biomass conversion yield $Y_{x/p}$, finding that this parameter is strongly dependent on the light stratification inside the reactor.

Acknowledgements□ Funds were provided by Universidad Nacional del Litoral, CAI + D Redes N°9 *Reactores y Procesos Biológicos para la Producción de Microorganismos Sustitutos de Agroquõmicos y para la Obtención de Materias Primas Alternativas para la Fabricación de Biocombustibles* and Consejo Nacional de Investigaciones Cientõficas y Técnicas de la República Argentina (CONICET) PIP IU *Modelado y optimización de foto-bio-reactores destinados al cultivo de microorganismos fototróficos para diferentes aplicaciones biotecnológicas.* The authors are grateful to Mr. Ramón A. Saavedra and Mr. Antonio Negro for providing technical support.

SUPPORTING INFORMATION

Additional Supporting Information may be found in the online version of this article:

Data S1. The expression for the probability of a collision between a photon and a bubble.

REFERENCES

1. Hu, Q., M. Sommerfeld, E. Jarvis, M. Ghirardi, M. Posewitz, M. Seibert and A. Darzins (2008) Microalgaltriacylglycerols as feedstocks for biofuel production: Perspectives and advances. *Plant J.* **54** (4), 621–639.
2. Jasvinder, S., Sai, G. (2010) Commercialization potential of microalgae for biofuels production. *Renew. Sustain. Energy Rev.* **14**, 2596–2610.
3. Brennan, L. and P. Owende (2010) Biofuels from microalgae—A review of technologies for production, processing, and extractions of biofuels and co-products. *Sust. Energ. Rev.* **14**, 557–577.
4. Bernard, O. (2011) Hurdles and challenges for modelling and control of microalgae for CO_2 mitigation and biofuel production. *J. Process Contr.* **21**, 1378–1389.
5. Fon Sing, S., A. Isdepsky, M. A. Borowitzka and N. R. Moheimani (2013) Production of biofuels from microalgae. *Mitig. Adapt. Strateg. Glob. Change* **18**(1), 47–72.
6. Mata, T. M., A. A. Martins and N. S. Caetano (2010) Microalgae for biodiesel production and other applications: A review. *Renew. Sust. Energ. Rev.* **14**, 217–232.
7. Raja, R., S. Hemaiswarya, N. A. Kumar, S. Sridhar and R. Rengasamy (2008) A perspective on the biotechnological potential of microalgae. *Crit. Rev. Microbiol.* **34**(2), 77–88.
8. Concas, A., M. Pisu and G. Cao (2010) Novel simulation model of the solar collector of BIOCOIL photobioreactors for CO_2 sequestration with microalgae. *Chem. Eng. J.* **157**, 297–303.
9. Concas, A., M. Pisu and G. Cao (2009) Novel simulation model of BIOCOIL photobioreactors for CO_2 sequestration. *Chem. Eng. Trans.* **17**, 1113–1118.
10. Kumar, K., C. N. Dasgupta, B. Nayak, P. Lindblad and D. Das (2011) Development of suitable photobioreactors for CO_2 sequestration addressing global warming using green algae and cyanobacteria. *Bioresour. Technol.* **102**(8), 4945–4953.
11. Spolaore, P., C. Joannis-Cassan, E. Duran and A. Isambert (2006) Commercial applications of microalgae. *J. BiosciBioeng.* **101**, 87–96.
12. Chojnacka, K. and A. Noworyta (2004) Evaluation of Spirulinasp.growth in photoautotrophic, heterotrophic and mixotrophicultures. *Enzyme Microb. Technol.* **34**, 461–465.
13. Perez-Garcia, O., F. M. E. Escalante, L. E. de-Bashan and Y. Bashan (2011) Heterotrophic cultures of microalgae: Metabolism and potential products. *Water Res.* **45**(1), 11–36.
14. Garcõa-Malea, M. C., F. G. Acién, J. M. Fernández, M. C. Cerón and E. Molina (2006) Continuous production of green cells of Haematococcuspluvialis: Modeling of the irradiance effect. *Enzyme Microb. Tech.* **38**, 981–989.
15. Perner-Nochta, I. and C. Posten (2007) Simulations of light intensity variation in photobioreactors. *J. Biotechnol.* **131**, 276–285.
16. Murphy, T. E. and H. Berberoglu (2011) Effect of algae pigmentation on photobioreactor productivity and scale-up: A light transfer perspective. *J Quant. Spectrosc. R. A.* **112**, 2826–2834.
17. Molina Grima, E., F. G. Acién Fernández, F. Garcõa Camacho and Y. Chisti (1999) Photobioreactors: Light regime, mass transfer, and scaleup. *J. Biotechnol.* **70**, 231–247.
18. Levert, J. M. and J. Xia (2001) Modeling the growth curve for Spirulina (Arthrospira) maxima, a versatile microalga for producing uniformly labelled compounds with stable isotopes. *J. Appl. Phycol.* **13**, 359–367.
19. Masojõdek, J., Š. Papácek, M. Sergejevová, V. Jirka, J. Cerveny, J. Kunc, J. Korecko, O. Verbovikova, J. Kopecký, D. Štys and G. Torzillo (2003) A closed solar photobioreactorfor cultivation of microalgae under supra-high irradiance: Basic design and performance. *J. Appl. Phycol.* **15**(2–3), 239–248.
20. Yun, Y. S. and J. M. Park (2001) Attenuation of monochromatic and polychromatic lights in *Chlorella vulgaris* suspensions. *Appl. Microbiol. Biotechnol.* **55**, 765–770.
21. Csőgör, Z., M. Herrenbauer, K. Schmidt and C. Posten (2001) Light distribution in a novel photobioreactor – modelling for optimization. *J. Appl. Phycol.* **13**(4), 325–333.
22. Heinrich, J. M., I. Niizawa, F. A. Botta, A. R. Trombert and H. A. Irazoqui (2012) Analysis and design of photobioreactors for microalgae production II: Experimental validation of a radiation field simulator based on a monte carlo algorithm. *Photochem. Photobiol.* **88** (4), 952–960.
23. Heinrich, J. M., I. Niizawa, F. A. Botta, A. R. Trombert and H. A. Irazoqui (2012) Analysis and design of photobioreactors for microalgae production I: Method and parameters for radiation field simulation. *Photochem. Photobiol.* **88**(4), 938–951.
24. Clescerl, L. S., A. E. Greenberg and A. D. Eaton (1999) Total Suspended Solids Dried at 103□105□C. In *Standard Methods for the*

Examination of Water and Wastewater (Edited by L. S. Clescerl, A. E. Greenberg, and A. D. Eaton), 20th edn. American Public Health Association, Washington, DC.
25. Ritchie, R. J. (2008) Universal chlorophyll equations for estimating chlorophylls a, b, c, and d and total chlorophylls in natural assemblages of photosynthetic organisms using acetone, methanol, or ethanol solvents. *Photosynthetica* **46**(1), 115–126.
26. Mendelson, H. D. (1967) The prediction of bubble terminal velocities from wave theory. *AIChE J.* **13**, 250.
27. Amol, A. K. and B. J. Jyeshtharaj (2005) Bubble formation and bubble rise velocity in gas-liquid systems: A review. *Ind. Eng. Chem. Res.* **44**, 5873–5931.
28. Vincenti, W. G. and C. H. Kruger (1967) *Introduction to Physical Gas Dynamics*, pp. 12–14. John Wiley & Sons, New York.